Published in
The European Physical Journal Applied (EPJAP) 388, issue 2, 183-189, 2007
which should be used for any reference to this work

An experimental study of intermodulation effects in an atomic fountain frequency standard

J. Guéna[a], G. Dudle, and P. Thomann[b]

METAS, Lindenweg 50, 3003 Bern-Wabern, Switzerland

Abstract. The short-term stability of passive atomic frequency standards, especially in pulsed operation, is often limited by local oscillator noise via intermodulation effects. We present an experimental demonstration of the intermodulation effect on the frequency stability of a *continuous* atomic fountain clock where, under normal operating conditions, it is usually too small to observe. To achieve this, we deliberately degrade the phase stability of the microwave field interrogating the clock transition. We measure the frequency stability of the locked, commercial-grade local oscillator, for two modulation schemes of the microwave field: square-wave phase modulation and square-wave frequency modulation. We observe a degradation of the stability whose dependence with the modulation frequency reproduces the theoretical predictions for the intermodulation effect. In particular no observable degradation occurs when this frequency equals the Ramsey linewidth. Additionally we show that, without added phase noise, the frequency instability presently equal to 2×10^{-13} at 1 s, is limited by atomic shot-noise and therefore could be reduced were the atomic flux increased.

1 Introduction

It is well established that the ultimate short-term stability of pulsed passive frequency standards can be limited by intermodulation effects, also known as the Dick effect [1, 2]. First described in the case of ion traps in 1987, the effect has regained interest with the development of cold cesium fountains [3], since most of these devices are operated with a pulsed scheme. The Dick effect arises from down-conversion of local oscillator frequency noise at even harmonics of the cycle rate into the fundamental frequency band of the locking loop, thereby degrading the achievable short-term stability. In a pulsed fountain one can make the effect negligible by employing a local oscillator exhibiting an ultra-high stability, such as a cryogenic sapphire oscillator [4,5]. An alternative route would be to ensure that at all times there are atoms between the two Ramsey pulses. One way to achieve this is to use a multipulse or a juggling atomic fountain [6,7]. The way we are currently pursuing is the *continuous* fountain approach. Rather than launching atoms in successive clouds, a such fountain produces a continuous beam of laser-cooled atoms.

Theoretical investigations, presented in a previous communication [8], have shown that intermodulation effects can also exist in a continuous fountain, albeit at a much lower level. But contrary to pulsed standards, they can be cancelled completely in the case of a continuous fountain if the modulation frequency of the interrogation is carefully selected; namely, if this frequency is an *odd* harmonic of the linewidth of the Ramsey resonance, the intermodulation effect cancels for any modulation scheme. In this paper we present an experimental verification of the suppression of the intermodulation effect in a continuous fountain when this condition is fulfilled and observe the degradation of the short-term stability when it is not. Results are compared with the theoretical prediction.

In Section 2, we present the experimental set-up used for this work, including a brief description of our continuous fountain, dubbed FOCS-1, and the frequency control loop. Section 3 is devoted to the present performances of FOCS-1 in terms of flux, signal-to-noise ratio and stability. In Section 4, we summarize the results of the model developed in [8] and use them to predict the intermodulation

[a] On leave from Laboratoire Kastler Brossel, ENS, Université Pierre et Marie-Curie-Paris 6, CNRS, 24 rue Lhomond, 75005 Paris, France.
Present address: LNE-SYRTE, 61 avenue de l'Observatoire, 75014 Paris, France.
e-mail: jocelyne.guena@obspm.fr
[b] LTF-IMT, Université de Neuchâtel, rue A.-L. Breguet 1, 2000 Neuchâtel, Switzerland.

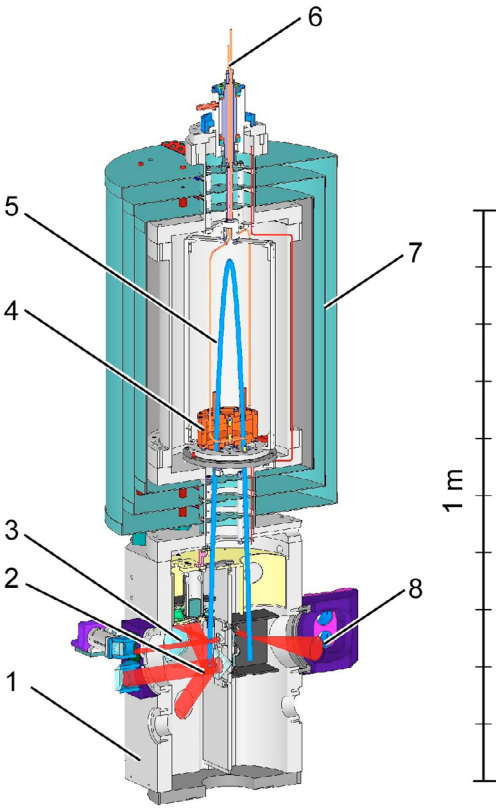

Fig. 1. Fountain set-up. 1: UHV chamber; 2: optical molasses capture region; 3: transverse cooling; 4: microwave cavity; 5: parabolic flight; 6: microwave field feedthrough; 7: magnetic shielding; 8: probe detection beam (the online version is in color).

effect in a realistic experiment. Measurements and results are presented in Section 5.

2 The continuous fountain clock set-up and interrogation method

2.1 Fountain set-up

Figure 1 shows a sketch of FOCS-1. A continuous 3D optical molasses (OM) captures atoms from the low velocity tail of a Cs vapor in an ultra-high vacuum chamber. The cold atoms are launched upwards with a longitudinal velocity of $\simeq$3.8 m/s using a moving molasses scheme (up- and down-going beams at 45° from the vertical, detuned by $\pm$3.2 MHz). The cold atom beam (isotropic temperature of about 60 μK) is transversally collimated by two orthogonal 1D optical molasses, which reduces the transverse temperature to about 7 μK. The cooling beams are tuned to the cross-over $F = 4 \rightarrow F' = 3 - F = 4 \rightarrow F' = 5$ of the $6S_{1/2}, F \rightarrow 6P_{3/2}, F'$ hyperfine transitions, i.e. 25 MHz to the blue side of the $F = 4 \rightarrow F' = 4$ component. A repumper beam tuned to the $6S_{1/2}, F = 3 \rightarrow 6P_{3/2}$, $F' = 4$ transition is superposed so that all atoms are cooled in the $F = 4$ ground state hyperfine level.

In the continuous fountain, the two Rabi interactions must be spatially separated. For this reason the transverse cooling plane is tilted by about 1.8° from horizontal and the atoms describe an open parabola with a flight duration $T \simeq 0.5$ s in between the two Rabi interaction zones (yielding a Ramsey fringe of $FWHM \simeq 1$ Hz). In the present set-up the cold atoms in $F = 4$ are partially pumped into $F = 3$ by the fluorescence light scattered by the OM source. Since this depumping is unavoidable, we have decided to complete the transfer into $F = 3$ by a transverse laser beam above the cooling plane resonant for $F = 4 \rightarrow F' = 4$. The remaining atoms in $F = 4$, $m_F \neq 0$ represent typically 40% of the population inversion of the clock transition $F = 3$, $m_F = 0 \rightarrow F = 4$, $m_F = 0$ and contribute noise.

The transit time in each Ramsey zone is of order 10 ms. A C-field $B \approx 70$ nT defines the vertical quantisation axis and lifts the degeneracy of the $F = 3$, $m_F \rightarrow F = 4$, m_F microwave transitions. After the second Rabi interaction, atoms in $F = 4$ only are detected by induced fluorescence on the $F = 4 \rightarrow F' = 5$ optical cycling transition. The detection efficiency limited by the solid angle of collection is a few percent. With a probe power 1.5 mW and waist diameter 10 mm, the number of photons detected per atom is $\gg$1, so that the detected shot noise is limited by atomic shot noise. The photodetector (Hamamatsu) with a feedback resistance 1 GΩ, has low dark noise (4×10^{-15} A Hz$^{-1/2}$). The output of the current-to-voltage converter is further amplified by a factor of 100.

2.2 Continuous Ramsey interrogation

A block diagram of the frequency control loop is shown in Figure 2. We start from a commercial voltage-controlled quartz crystal oscillator VCXO (BVA 8607 from Oscilloquartz) which displays an Allan deviation of 10^{-13} up to 100 s. A frequency synthesiser upconverts the 10 MHz output of the VCXO to 9180 MHz with a phase modulation at 12.6 MHz provided by an external generator (HP3325 synthesiser). This generates the microwave field with a carrier frequency at the clock transition frequency (9 192 631 770 Hz) and an amplitude adjusted to induce $\pi/2$ Rabi pulses in the Ramsey cavity. To produce an error signal for the frequency corrections, the *phase* of the 12.6 MHz oscillation issued from the HP3325 synthesiser is square-wave modulated with a p.p. amplitude of $\pi/2$. The phase of the microwave field at the clock frequency is thus modulated with the same waveform and amplitude. The waveform, frequency f_{mod} and amplitude of the phase modulation are controlled by the reference output of a digital lock-in amplifier (DLA). The fluorescence photodetector signal is square-wave demodulated in the DLA, integrated and the correction voltage applied to the VCXO. The locking loop is controlled by a Labview software routine.

3 Signal-to-noise and present clock stability

In a continuous fountain, if all technical noise sources can be suppressed sufficiently, the achievable stability is

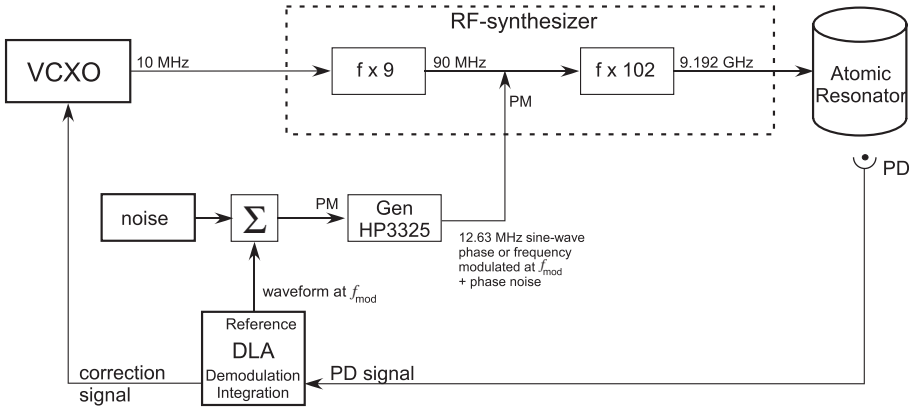

Fig. 2. Block diagram of the frequency control loop. VCXO: voltage-controlled quartz crystal oscillator; PD: fluorescence photodetector. DLA: digital lockin amplifier. Gen: RF synthesiser. PM: phase modulation. The use of the noise generator (noise) and summing amplifier Σ is detailed in Section 5.

limited only by the signal-to-noise ratio S/N of the detected atomic flux which itself scales with the square root of this flux (atomic shot noise limit). The Allan deviation σ_y, a measure of the frequency instability of the fountain, is then expected to scale with the inverse square root of the atomic flux, $\sigma_y \propto \phi^{-1/2}$. To verify that our fountain satisfies these conditions, we have first measured the noise as a function of the atomic flux.

For these measurements, the atomic flux was varied in two independent ways, either (i) by changing the power of the repumper laser or (ii) by modifying the power of the cooling beams of the 3D-optical molasses. The fluorescence photodetector signal was spectrum analysed (Stanford Research Systems SR760 FFT). The noise was observed to be white between 0.1 Hz and 20 Hz with a dominant contribution from atomic fluorescence, as can be seen in an example of a recording shown in Figure 3a. Figure 3b displays the measured noise as a function of the detected atomic flux for both methods. The small noise contribution from the background signal due to scattered probe light ($\sim 5 \times 10^{-15}$ A Hz$^{-1/2}$) has been subtracted quadratically. The experimental data are fitted with a power law $N = S^k$ where N represents the noise and S the atomic signal. The value obtained for k lies $\sim 2.5\sigma$ above the value 0.5 expected for pure atomic shot noise.

From the signal-to-noise ratio one can also deduce the number of detected atoms. Indeed, it can readily be shown that the atomic flux is related to the signal-to-noise ratio by $\phi = 2\,(S/N)^2$.

Using this equation, we infer that for the data point corresponding to the strongest atomic signal, the useful flux[1] is of order 2×10^5 at/s.

For the frequency stability measurements, the 10 MHz output of the VCXO locked to the fountain is compared with the 10 MHz output of a maser contributing to the definition of TAI (maser 140-57-01) using a frequency comparator (VCH-314). Figure 4 displays a typical result obtained at maximum flux. At 1 s, the phase noise of the maser dominates. For $\tau > 200$ s, the Allan deviation is consistent with $2 \times 10^{-13}\tau^{-1/2}$ and lies near the limit $\sim(1.5 \text{ to } 1.8) \times 10^{-13}\tau^{-1/2}$ associated with the atomic shot noise expected from the signal-to-noise ratio discussed

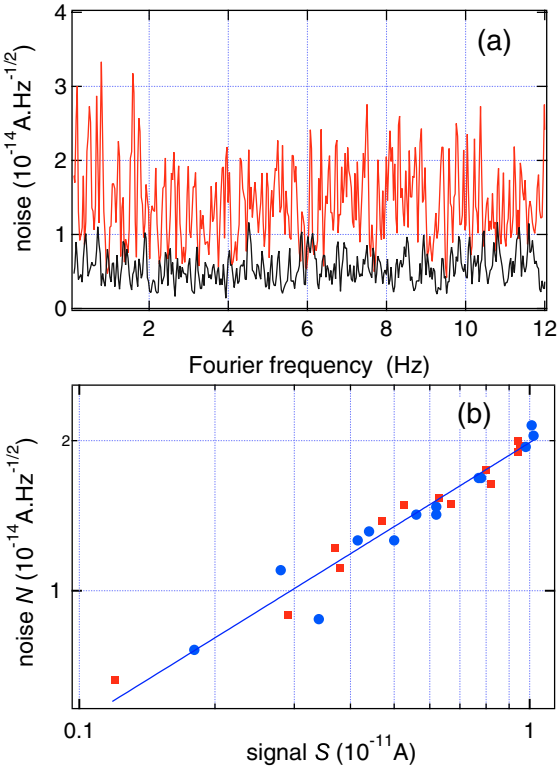

Fig. 3. Rms values of the noise N of the fluorescence photodetector signal. (a) *vs* the Fourier frequency at intermediate atomic flux (upper trace) and without atomic flux (lower trace). (b) *vs* the contribution S of the atomic fluorescence to the DC signal. The microwave field is tuned to the centre of the central Ramsey fringe of the clock transition without phase modulation. The atomic flux is varied by varying the power of the repumper beam (squares) or of the cooling beams (bullets) in the 3D-optical molasses source. The straight line is a fit by a power law with exponent 0.560 ± 0.025.

[1] This is the flux of atoms having undergone the clock transition excluding the background atoms in $F = 4$, $m_F \neq 0$.

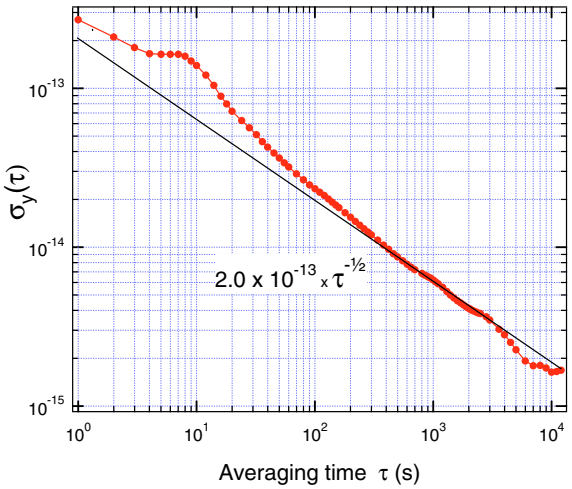

Fig. 4. Allan deviation σ_y of the LO locked to FOCS-1 compared to the reference maser, as a function of the averaging time τ. The points represent the experimental data and the continuous line indicates $2.0 \times 10^{-13}\ \tau^{-1/2}$.

above. In addition, control measurements performed at half-maximum flux were consistent with a degradation of the instability as $\phi^{-1/2}$, i.e. with atomic shot noise.

4 The predicted intermodulation effect

4.1 Allan deviation due to the intermodulation effect

A theoretical analysis of a possible degradation of the frequency stability of a frequency standard due to intermodulation effects has been presented in detail previously [8]. Here, only the basic ingredients of the model and the main results will be recalled.

From a knowledge of the power spectral density (PSD) of the frequency fluctuations of the free running oscillator $S_y^{LO}(f)$, the model aims at predicting the power spectral density $S_y^{LLO}(f)$ of the oscillator locked to a Ramsey resonator using any modulation–demodulation scheme. Though the treatment was developed specifically for the case of a continuous interrogation, it can also be applied to the pulsed case, or for that matter, to any-time dependence of the atomic flux. From the PSD of the locked oscillator, the Allan deviation can then readily be computed.

The spectrum of the LLO has two parts: the first corresponds to the error signal that controls the LO frequency fluctuations; the second, not reduced by the loop gain, contains all *even* harmonics of the modulation frequency f_{mod} and corresponds to a spurious signal generated by down-conversion of the LO frequency fluctuations at harmonics of the modulation frequency. The latter is the aliasing part of interest here and is given by equation (30) of reference [8]:

$$S_{y,Dc}^{LLO}(f) \simeq 2\sum_{k=1}^{\infty} \frac{|c_{2k}|^2}{c_0^2} \mathrm{sinc}^2(2k\pi f_{mod} T) S_y^{LO}(2k f_{mod}) \tag{1}$$

for Fourier frequencies $0 \leq f \leq f_F$, where sinc $(x) = \sin(x)/x$, the c_{2k} are the Fourier coefficients of the modulation-demodulation function, T is an effective transit time between the two Ramsey pulses (here $\simeq$0.49 s) and f_F is the bandwidth of the low-pass filter in the loop. A remarquable property of this equation is that for the condition $T = T_{mod}/2$, i.e. when the modulation frequency is equal to the resonator linewidth $\Delta\nu_0$ ($\simeq$1 Hz), all terms in equation (1) are equal to zero: as a result the aliasing effect vanishes, whatever modulation-demodulation scheme. The interpretation is a filtering effect of the LO frequency fluctuations at the even harmonics of f_{mod} by averaging over the transit time through the resonator. In the particular case of square-wave phase modulation and square-wave demodulation the c_{2k} vanish for all values of k, which provides an even more robust cancellation effect.

The bandwidth of the frequency control loop f_F is a fraction of a hertz. Within this bandwidth, the frequency perturbations $S_{y,Dc}^{LLO}(f)$ due to the continuous intermodulation effect can be considered as white noise (Eq. (1)). As a consequence, the Allan deviation due to this effect is given by:

$$\sigma_{y,Dc}^2(\tau) = S_{y,Dc}^{LLO}(f=0)/2\tau \tag{2}$$

provided the averaging time τ is longer than the time constant of the servo loop (typically $\tau > 10$ s).

For quantitative predictions, we must calculate the Fourier coefficients c_{2k} involved in equation (1) and use a model for $S_y^{LO}(f)$, the PSD of the frequency fluctuations of the free LO. For $S_y^{LO}(f)$, the main sources of frequency instability can be parametrized by the following expansion:

$$S_y(f) = \sum_{\alpha=-2}^{2} h_\alpha \times f^\alpha \tag{3}$$

corresponding to random frequency (h_{-2}), flicker frequency (h_{-1}), white frequency (h_0), flicker phase (h_1) and white phase noise (h_2).

In reference [9], three usual types of modulation schemes were investigated: square-wave phase modulation, sinusoidal-wave and square-wave frequency modulations, and, for each of them, either first harmonic or wideband demodulation schemes were considered. The simulations of the intermodulation effect were performed for a particular quartz oscillator exhibiting contributions from h_{-1} and h_1 types of noise, with a flicker floor Allan deviation of 3×10^{-13}. The results show that for significant deviation (0.4 to 0.5 Hz) of f_{mod} from the value $\Delta\nu_0 = 1$ Hz (or its odd harmonics) the Allan deviation due to the intermodulation effect reaches at most 10^{-13} for $\tau = 1$ s, that is, a value below the present Allan deviation limited by the atomic shot noise (see Sect. 3 where f_{mod} is chosen equal to $\Delta\nu_0 = 1$ Hz). Similar results were obtained with the three modulation schemes[2]. Since our present oscillator is

[2] We note that differences between the different modulation schemes show up essentially in how the effect vanishes in the vicinity of $f_{mod} = \Delta\nu_0$. Of course, for optimum performances of the clock under normal operation these differences have to be considered and the best modulation scheme adopted.

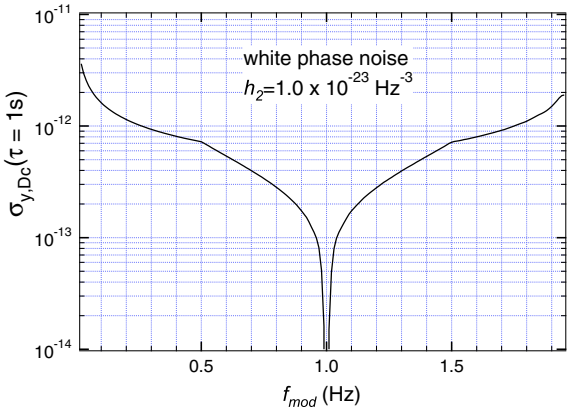

Fig. 5. Allan deviation due to the intermodulation effect using the model developed in [8] for the case of square-wave phase modulation with white phase noise $h_2 = 10^{-23}$ Hz^{-3}, as a function of the frequency modulation f_{mod}. Values calculated for an averaging time $\tau = 1$ s.

even better with a ∼3 times lower flicker phase noise, it is not well suited for demonstrating the intermodulation effect. It was thus necessary to degrade deliberately the phase noise performance of the LO. We chose to inject white phase noise (h_2-type) with an amplitude such that the intermodulation effect contribution is ∼2 times the atomic shot noise for an experimentally sensible deviation of f_{mod} from 1 Hz (or its odd harmonics).

4.2 Prediction in the case of square-wave phase modulation with white phase noise

For square-wave phase modulation and wideband demodulation, the Fourier coefficients can be calculated analytically, and from equation (6.32) of reference [9] the h_2 contribution to the intermodulation effect reads:

$$\sigma_{y,Dc}(\xi,\tau) = \frac{1}{2\pi^2\xi(1-|\xi-1|)}\left\{\frac{h_2}{T^2}\,\xi^2\,g(\xi)\right\}^{1/2}\tau^{-1/2} \quad (4)$$

where $g(\xi) = \sum_{k=0}^{\infty}\sin^4(k\pi\xi)/k^2$ and $\xi = f_{mod}\,/\Delta\nu_0$. The dependence of the Allan deviation on the frequency modulation f_{mod} is shown in Figure 5 for $h_2 = 10^{-23}$ Hz^{-3}. Using the relation $S_\phi(f) = S_y(f) \times (f_0/f)^2$ with $f_0 \simeq 9.2$ GHz the clock frequency, this corresponds to a PSD of the phase noise $S_\phi(f)$ of 10^{-3} rad^2 Hz^{-1}. One can see the notch effect of the continuous Ramsey resonator at 1 Hz, the width $\Delta\nu_0$ of the resonance line, and the rapid degradation either side of this value.

5 Noise generation, measurements and results

To generate the phase noise in the microwave field, we add a noise voltage to the phase modulation input of the 12.6 MHz generator (see Fig. 2). The noise voltage provided by a wideband white noise generator (DS340) is low-pass filtered and amplified beforehand. We adjust the cut-off frequency to select the first 20 harmonics of the modulation frequency f_{mod}, since these give almost the whole contribution (>98%) to the intermodulation effect. The rms noise voltage is adjusted to provide a phase noise of order ∼30 mrad Hz$^{-1/2}$ ($h_2 \approx 10^{-23}$ Hz^{-3}). Note the interest of injecting the phase noise into the 12.6 MHz oscillation, rather than directly into the VCXO control voltage input: the added frequency instability of the VCXO is then representative of the intermodulation effect, and not of some parasitic effect due to a direct degradation of the VCXO.

Most of the frequency stability measurements were performed using square-wave phase modulation with f_{mod} varied around either 1 Hz or 3 Hz, i.e. the first or third harmonic of the Ramsey resonator linewidth. The Allan deviations, for each value of f_{mod}, obtained after a measurement time of typically 2 hours are plotted in Figures 6a and 6b, respectively. For τ of a few hundred seconds, the VCXO is locked to the fountain and the Allan deviations approach the $\tau^{-1/2}$ law (white frequency noise) expected from both atomic shot noise and the intermodulation effect. For $\tau > 1000$ s, the statistics are poorer and the values less significant. We should note that, when the modulation frequency is changed, the slope of the Ramsey discriminator also changes. For instance with $f_{mod} = 1.4$ Hz, the slope is decreased by 30% in square-wave phase modulation mode[3]. This means that even in the absence of the intermodulation effect, the stability limited by the atomic shot noise can be degraded when f_{mod} is varied. This effect has been taken into account by our repeating the measurements without phase noise injected in the synthesiser. The observed degradation due to the change of the discriminator slope agrees with that expected based on atomic shot noise and remains much smaller than the frequency instability observed when phase noise is injected (see below). Measurements were also performed using square-wave *frequency* modulation. Simulations carried out in reference [9] indicate that the intermodulation effect should show up with the same order of magnitude. In this case the slope is smaller as is its dependence on f_{mod}. The experimental results are plotted in Figure 6c. In the three graphs of Figure 6, the better stability obtained at f_{mod} equal to 1 Hz (in Figs. 6a and 6c) or 3 Hz (in Fig. 6b) is quite conspicuous.

With a view to extracting the intermodulation contribution to the measured instabilities and comparing them with the prediction above, we subtracted quadratically the instabilities measured without injected phase noise from the total instabilities measured in presence of phase noise. The values are taken for averaging times τ in the range 100 to 400 s and scaled to 1 s using the $\tau^{-1/2}$ law. The results are plotted as a function of f_{mod} in Figure 7. There is good agreement with the calculated intermodulation effect. The

[3] The phase of the demodulation has also to be readjusted, which is done by maximizing the Ramsey slope when the microwave frequency is detuned by a half linewidth (±0.5 Hz) from the fringe centre.

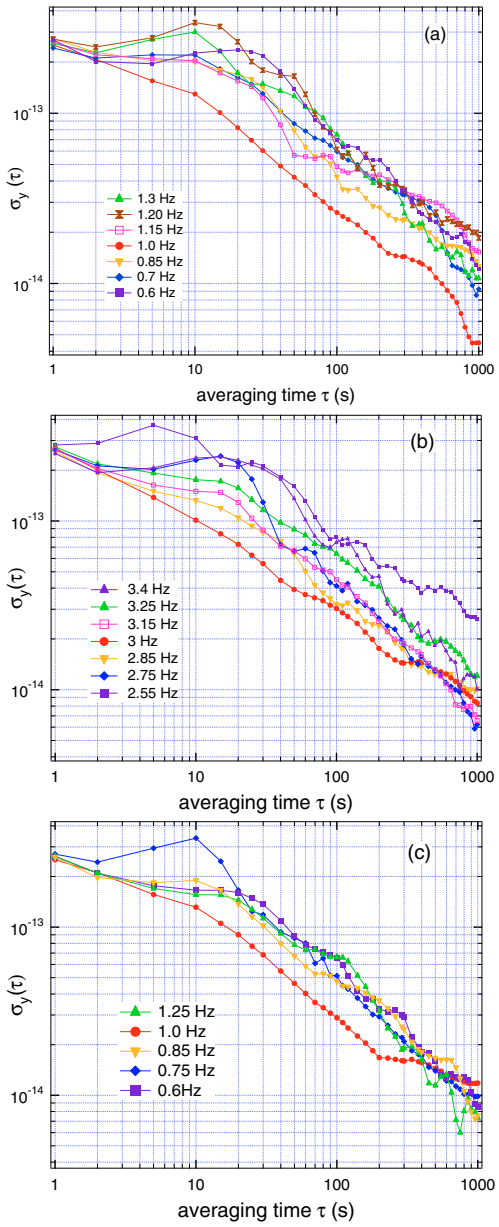

Fig. 6. Experimental Allan deviations of the LO locked to FOCS-1 with white phase noise injected *via* the synthesiser into the microwave field fed to the Ramsey resonator. (a) Square-wave phase modulation with modulation frequency varied around 1 Hz, the ($FWHM$) linewidth of the resonator. (b) Square-wave phase modulation with modulation frequency varied around 3 Hz. (c) Square-wave frequency modulation with modulation frequency varied around 1 Hz (the online version is in color).

most important feature is the suppression of the effect when the modulation frequency equals an *odd* harmonic of the Ramsey fringe linewidth. Note that we have used the model of reference [8] which makes several simplifications, namely: monokinetic atomic beam; infinitely short Rabi pulses, hence absence of transients; no phase shift between modulation and demodulation waveforms. One might reasonably enquire whether these idealizations could yield

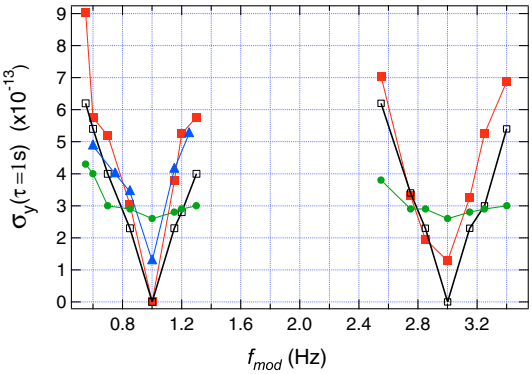

Fig. 7. Allan deviations vs. interrogation modulation frequency: observed in square-wave phase modulation without injected phase noise, used as references (bullets); observed with injected phase noise after quadratic subtraction of the references (filled squares and triangles for square-wave phase and square-wave frequency modulations, respectively); predicted intermodulation effect for injected noise $h_2 = 10^{-23}$ Hz^{-3} and square-wave modulation (open squares) (the online version is in color).

an underestimate of the effect. However, several points involved in the real experiment were considered in reference [9]: (i) longitudinal velocity distribution of atoms (a few cm/s around the average launch velocity of 4 m/s, or longitudinal temperature of about 75 μK); (ii) phase shift between modulation and demodulation; (iii) introduction of dead times (blanking) of duration equal to the duration of the transients. From these simulations, the corresponding degradations of stability are expected to be very small compared with the atomic shot noise. Thus we believe that the observed slight excess of instability over the predicted value arises from some technical noise added in the generation of the phase noise[4]. We recall that the latter corresponds to an increase by 2 to 3 orders of magnitude with respect to the undegraded phase noise, and to an rms phase noise of 2% of the $\pi/2$ p.p. phase modulation. Concerning the possible effect of transients, we note that these could show up when f_{mod} is varied around 3 Hz instead of 1 Hz. In fact, no significant degradation is observed (see Fig. 7).

6 Conclusion

In this paper, we show that a continuous cold-atom fountain clock that uses a commercial quartz crystal oscillator has a frequency stability limited mainly by atomic shot noise. By deliberately degrading the noise spectrum of the microwave field fed to the Ramsey cavity, we have verified the model specifically developed to predict the intermodulation effect in a continuous interrogation scheme,

[4] We note that for some values of f_{mod}, oscillations of the LO frequency with a long period (in the range 100 to 2000 s) appeared. However, they were not reproduced with a second noise generator (DS345) whose algorithm to generate random noise is different. This highlights just how hard it is to generate perfectly white noise without adding side effects in the loop.

in particular the cancellation of this effect when the modulation frequency involved in the microwave frequency locking loop equals an odd harmonic of the resonator linewidth ($FWHM \simeq 1$ Hz). The magnitude of the effect when the modulation frequency is changed from these values is observed at the level predicted by the model. This experimental verification is important because several points involved in the actual experiment, e.g. transients effects, are difficult to include in the model. To observe the intermodulation effect at a level comparable with that of the present atomic shot noise, we were led to degrade the noise of our quartz oscillator by 2 to 3 orders of magnitude. This work thus demonstrates the advantage of the continuous fountain approach in reducing intermodulation-related local oscillator noise and opens the possibility of improving significantly the short-term stability of a continuous fountain by increasing the atomic flux.

We wish to thank M.D. Plimmer for critical reading of the manuscript. METAS acknowledges the Centre National de la Recherche Scientifique (CNRS) and Laboratoire Kastler Brossel, unité mixte de recherche (UMR 8552) of the CNRS, for having made possible the stay of J.G. at its institute.

References

1. G.J. Dick, in *Proceedings of the 19th Precise Time and Time Interval meeting (PTTI), Redendo Beach, CA, 1997*, pp. 133–147
2. G.J. Dick, J.D. Prestage, C.A. Greenhall, L. Maleki, in *Proceedings of the 22nd Precise Time and Time Interval meeting (PTTI), Vienna, VA, 1990*, pp. 487–508
3. G. Santarelli, C. Audoin, A. Makdissi, Ph. Laurent, G.J. Dick, A. Clairon, IEEE Trans. Ultrason. Ferroelectr. Freq. Control **45**, 887 (1998)
4. G. Santarelli, P. Lemonde, Ph. Laurent, A. Clairon, A.G. Mann, C. Sheng, A.N. Luiten, C. Salomon, Phys. Rev. Lett. **82**, 4619 (1999)
5. A.G. Mann, C. Sheng, A.N. Luiten, IEEE Trans. Instrum. Meas. **50**, 519 (2001)
6. S. Ohshima, T. Kurosu, T. Ikegami, Y. Nakadan, in *Proceedings of the 5th Symposium on Frequency Standards and Metrology, Woods Hole, Massachussets* (World Scientific Singapore, 1995), pp. 60–65
7. R. Legere, K. Gibble, Phys. Rev. Lett. **81**, 5780 (1998)
8. A. Joyet, G. Mileti, G. Dudle, P. Thomann, IEEE Trans. Instrum. Meas. **50**, 150 (2001)
9. A. Joyet, Ph.D. thesis, University of Neuchâtel, 2003, `http://www.unine.ch/biblio/bc/cyber\_liste\_fac \_inst\_FS\_physique.html`